Technical University of Denmark

DTU

D2 dissociative adsorption on and associative desorption from Si(100): Dynamic consequences of an ab initio potential energy surface

Luntz, A. C.; Kratzer, Peter

DTU Library
Technical Information Center of Denmark

D$_2$ dissociative adsorption on and associative desorption from Si(100): Dynamic consequences of an *ab initio* potential energy surface

A. C. Luntz[a)]
IBM Research, Almaden Research Laboratory, San Jose, California 95120

P. Kratzer
Center for Atomic-scale Material Physics and Physics Department, Technical University of Denmark,
DK-2800 Lyngby, Denmark

Dynamical calculations are reported for D$_2$ dissociative chemisorption on and associative desorption from a Si(100) surface. These calculations use the dynamically relevant effective potential which is based on an *ab initio* potential energy surface for the ''pre-paired'' species. Three coordinates are included dynamically; the distance to the surface, the D–D bond length and a Si phonon coordinate. Other coordinates (multidimensionality) have been included via a static approximation. Both an asymmetric and symmetric reaction paths are considered. While energetics favors the asymmetric path, phase space favors the symmetric one. Under the conditions of many experiments, either could dominate. The calculations show quite weak dynamic coupling to the Si lattice for both paths, i.e., weak surface temperature dependences to dissociation and small energy loss to the lattice upon desorption. These calculations do not support previous suggestions that either a strong coupling to the lattice or ''entropic'' effects can reconcile the apparent violation of detailed balance obtained by comparing experimental dissociation to desorption barriers. In fact, the results reported here do not agree with several experimental findings. We discuss several possibilities for this disagreement, including experimental artifact, limitations in the dynamical model and even the possibility that electronically adiabatic dynamics involving the ''pre-paired'' species is not relevant to experiments on real systems. © *1996 American Institute of Physics.* [S0021-9606(96)00808-4]

I. INTRODUCTION

Hydrogen terminated Si surfaces have been well studied within the surface science community for many years. In part, this is due to their technological importance in passivating Si. Recently, the kinetics and dynamics of hydrogen dissociation on and desorption from Si(100) have initiated considerable new discussion and debate. The initial motivation for this renewed interest was the finding that the kinetics of associative desorption followed first-order rather than second-order kinetics.[1,2] This observation has stimulated a rather lively debate as to the underlying mechanism. The most generally accepted rationale for this currently is that desorption occurs from a ''pre-paired'' configuration,[3] although defect mediated desorption has also often been invoked.[4–6] There is now some experimental[2] and considerable theoretical support[7,8] that the ''pre-paired'' state is a minimum energy configuration. This does not, however, guarantee that the first-order kinetics is due to desorption through this configuration. One of the principal reasons that defect models have been suggested to explain the first-order kinetics is that the energetics of desorption from some *ab initio* cluster calculations[4–6] was found to be larger than experimental measurements. While these calculations did allow some substrate relaxation, other *ab initio* cluster calculations employing more substrate relaxation[9] as well as several *ab initio* slab calculations[10–12] are in agreement with experimen-

tal desorption energies, so that this argument must be viewed with some caution. It should also be pointed out, however, that both of the latter sets of calculations are based on density functional theory, while the former are all based on configuration interaction so that this may also play a significant role in the contradictory results.

More recently, another puzzle has provoked even more controversy, i.e., trying to reconcile associative desorption from the monohydride phase of Si(100) with measurements of dissociative chemisorption. Populations of internal states of H$_2$ and D$_2$ thermally desorbed from Si(100) have been measured via laser spectroscopy.[13] Desorbing species were found to be rotationally cold and only weakly vibrationally excited. Recent laser induced thermal desorption experiments also show that desorbing D$_2$ is translationally equilibrated at the surface temperature,[14] i.e., cold as well. Combining these two experiments implies that the barrier to adsorption should be quite small.[15] In contrast, all measurements of dissociative chemisorption of H$_2$ and D$_2$ on Si(100) find that the magnitude for this sticking is very small,[15–17] consistent with a high barrier to dissociation. Since the barrier to dissociation and desorption should be equivalent, the incompatibility in the two barrier determinations has been discussed in terms of an apparent violation of detailed balance.[15]

Many ideas have been suggested to reconcile the low sticking coefficient with the desorption data. In addition to the rather obvious possibility of the importance of defects in one or both processes, several *ad hoc* models have also been

suggested for the "pre-paired" configuration. For example, it has been postulated that tunneling through a barrier is important. In such a scenario, desorbing species do not reflect the high barrier since they have tunneled through it, but the sticking could still be low and show strongly activated behavior.[18] Another key experimental finding is that the sticking is activated by surface temperature,[15,19,20] although the magnitude of the activation observed in two experiments is qualitatively different. The observed temperature dependence is thought to be related to the fact that the adsorption of hydrogen involves major structural relaxations of the Si(100) surface, i.e., that the Si dimers on the clean surface are strongly buckled relative to the surface normal while the monohydride surface of Si(100) consists of symmetric flat dimers. Based on this, Brenig and co-workers[21] suggested that a quite high barrier exists, but that it is located mainly in the degrees of freedom of the Si substrate. Due to a strong coupling between desorption and substrate relaxation in their model, the energy released after traversing the barrier is transferred mainly to the surface atoms. Hence the molecules desorb with little kinetic energy, while the surface remains in a highly excited state after desorption. Others[15,11,22] have suggested that the barrier for sticking could be partly entropic in nature, i.e., a result of the high dimensionality of the dissociation process. Only a few orientations and impact parameters of the molecule and few surface configurations are favorable for sticking, and this results in a small sticking coefficient. The desorption is assumed to proceed predominantly via the lowest possible barrier, involving full substrate, impact parameter and orientational relaxation and therefore with little excess energy available for the desorbing molecules.

Recently, a detailed mechanism for the adsorption and desorption of H_2/Si(100), involving a "pre-paired" state, has been suggested on the basis of *ab initio* density functional calculations.[9–12,23] The lowest energy pathway between the adsorbed (monohydride) and gas phase H_2 or D_2 is via an asymmetric transition state. This transition state occurs for a Si dimer buckling angle intermediate between that of the free surface and the flat dimer appropriate for the monohydride surface. It has been argued[10,11,23] that such a PES topology can qualitatively reconcile many of the dynamical observations. Using a "sudden" approximation for sticking, it was suggested that an incoming H_2 or D_2 sees a "frozen" Si dimer configuration characteristic of the free lattice and for which the barrier to dissociation is high. On the other hand, associative desorption is taken to be a slow adiabatic process which always finds the minimum energy pathway and thus a much lower barrier. It is therefore suggested that such a PES is compatible with the experimental finding of a high barrier in dissociative adsorption and a low barrier for associative desorption. In addition, since the barrier depends significantly on the Si dimer angle, this provides a mechanism for coupling of the H_2 or D_2 to substrate phonons and could result in both energy loss to the substrate in desorption and a temperature dependence of the dissociative chemisorption. Thus, this PES was taken as partial justification for key as-

pects of the models of both Brenig and co-workers[21] and Kolasinski *et al.*[15]

In an effort to strengthen the connection between the *ab initio* PES and experimental observations, we have performed dynamical simulations of D_2 dissociative chemisorption and associative desorption on models of the dynamically relevant effective potentials based on the *ab initio* PES. These simulations included three dimensions dynamically, in which the full coupling to a Si dimer phonon is included, while other coordinates are treated statically. Although many of the qualitative features discussed above do arise in the dynamical calculations, the effects are far weaker than suggested in previous interpretations of the experiments. For example, only a modest surface temperature dependence is predicted for dissociative chemisorption and very small energy transfer to the lattice upon desorption. We thus conclude that adiabatic dynamics based on the *ab initio* PES *cannot* account for the experimental results, nor resolve the dynamical paradox between dissociation and desorption. Several possible reasons for this disagreement are discussed, including experimental artifact, incomplete or inaccurate theoretical treatments and the possibility that other physical effects entirely dominate in experiments on real surfaces.

Even though the asymmetric transition state is the minimum energy path for dissociation or desorption, a somewhat higher energy path involving a symmetric transition state was also found in the *ab initio* calculations.[23] Because dynamics based on a PES involving the asymmetric transition state gave such poor agreement with experiment, we have also performed dynamical calculations for the effective potential based on an *ab initio* PES about the symmetric path as well. We find weak dynamic coupling of the D_2 to the Si dimer phonons on this PES as well. Although this is a higher energy path, the symmetric path is favored both in terms of phase space and for higher T_s, so that this path may be important in dissociation and desorption as well as the asymmetric one.

The rest of the paper will be organized as follows: Section II gives a brief overview of the PES and previews the dynamics via the application of transition state theory, Sec. III discusses the general dynamical procedure, Sec. IV discusses the *ab initio* PES, Sec. V presents the models of the dynamically relevant effective potentials, Sec. VI presents dynamical calculations of dissociative chemisorption, Sec. VII presents dynamical calculations of associative desorption, Sec. VIII gives a comparison of the dynamical calculations to existing experiments and suggests possible reasons for the poor qualitative agreement and Sec. IX gives a brief summary and some conclusions. Appendix A presents the definition of a reduced dimensionality dynamical model in terms of the full multidimensionality and defines the dynamically relevant effective potential to be used in such a case. Simple approximations to include multidimensionality statically are also discussed there.

II. TRANSITION STATE THEORY

As a prelude to discussing the dynamics, we summarize the results of the density functional calculations of Ref. 23 as
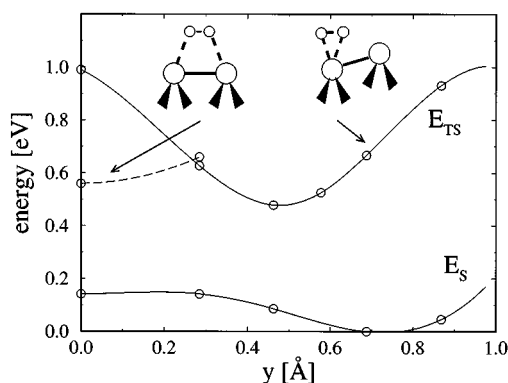
FIG. 1. Total energy of the asymmetric and symmetric transition states E_{TS} for D_2 interacting with Si(100) and of the clean surface E_s as a function of the Si dimer phonon coordinate Y.

TABLE I. The normal modes of the D_2 molecule at the asymmetric and the symmetric transition state. The labels are chosen as a hint to what the mode resembles most closely. The missing entry is the main component of the reaction coordinate.

Normal mode	Asymmetric TS $\hbar\omega$ [meV]	Symmetric TS $\hbar\omega$ [meV]
Reaction coordinate	$i92$	$i134$
D–D stretch	127	184
Si–D_2 stretch	71	⋯
Hindered cartwheel	117	81
Hindered helicopter	67	57
Translation parallel to dimer	⋯	11
Translation normal to dimer	32	3.5
Sum of real modes	414	336

follows (see Fig. 1): The lowest energy pathway between gas phase D_2 and dissociatively adsorbed D atoms on Si(100) involves an asymmetric transition state located above the lower Si atom of the buckled Si dimer. Displacements of the Si atoms modify the barrier height for adsorption. The most important excitation in this regard is a surface phonon mode where bond lengths are relatively unchanged, but the lower Si atom (principally) moves due to changes in the degree of buckling of the Si dimer. We have introduced a generalized coordinate Y to describe the displacement of the lower Si atom in the Si dimer relative to the flat dimer in the monohydride. The energy of the clean surface as a function of Y (lower curve in Fig. 1) shows the well-known minimum at the buckled-dimer reconstruction. The barrier height for adsorption, (upper curve in Fig. 1), however, has its minimum for a less buckled configuration of the Si dimer. A barrier of 0.48 eV for adsorption was obtained for the asymmetric transition state. More extensive calculations reported here (larger surface supercell) yield a lower barrier of 0.24 eV. The regime where the dimer is almost flat has a completely different transition state; one where the D_2 center of mass is midway between the two Si atoms of the flat dimer (dashed line in Fig. 1). For this transition state, a barrier of 0.57 eV was obtained earlier and which increased negligibly to 0.59 eV in the larger supercell calculations reported here. A normal mode analysis has also been performed for both of these transition states[23] and is presented in Table I.

Although the barrier through the asymmetric transition state is lower, it is not immediately apparent that this path will be dominant in actual experiments because this neglects all phase space considerations. For example, in dissociative adsorption, we would anticipate that the asymmetric transition state dominates for collisions where the impact parameter is near the lower Si atom of the dimer pair. On the other hand, for impact near the center of the dimer pair, we anticipate that the symmetric transition state is dominant. Which transition state is the best description for intermediate impact parameters depends in large extent to the phase space available around these two limits.

Given only the barrier heights and normal mode frequen-

cies at the saddle point, transition state theory (TST) provides reasonable estimates of thermal rate constants. The application of TST to dissociative adsorption and associative desorption has been widely discussed in the literature (see for example Weinberg[24]). While not taking absolute TST rates too seriously, the relative rates should provide a reasonable estimate of the importance of the two transition states since they depend *both* on barrier height *and* phase space. The ratio of the two TST rates for adsorption and desorption is given as

$$\frac{k_{\text{sym}}}{k_{\text{asym}}} = e^{-(\Delta U_{\text{sym}} - \Delta U_{\text{asym}})/k_B T_s} \frac{\Pi q_i^{\pm}(\text{sym})}{\Pi q_i^{\pm}(\text{asym})}. \qquad (1)$$

ΔU_X is the zero point corrected barrier for the transition state X, i.e., $\Delta U_X = V_X^* + 0.5(\Sigma \hbar \omega_i^{\pm} - \Sigma \hbar \omega_i)$ where V_X^* is the barrier on the PES and $\omega_i^{\pm}$ and ω_i are the vib rationale frequencies at the transition state and in the reactant respectively for all normal modes i in X. $q_i^{\pm}(X) = (1 - e^{-\hbar\omega_i^{\pm}/k_B T_s})^{-1}$. The first term in the ratio of Eq. (1) is the effect of the different zero point corrected barriers for the two transition states and the second term reflects the importance of the vibrational phase space of each.

Using the barrier heights from *ab initio* calculations with the $c(4 \times 2)$ surface unit cell (0.24 and 0.59 eV) and the vibrational frequencies of Table I, and assuming a $T_s = 950$ K typical of laser desorption experiments, this ratio $k_{\text{sym}}/k_{\text{asym}} = 0.03 \times 46. \approx 1$. Thus, although the barrier strongly favors the asymmetric path, phase space strongly favors the symmetric path. The latter is due to the much lower vibrational frequencies for the hindered translations in the symmetric relative to the asymmetric transition states. Since these two effects largely offset each other, it is virtually impossible to predict which transition state is most important in thermal rates.

Because of the possibility that either transition state may dominate adsorption or desorption, we have calculated dynamical processes through both paths in order to assess the compatibility of both with experiments.

III. DYNAMICAL MODELS: GENERALITIES

A full adiabatic description of D_2 dissociation and desorption from Si(100) is given in terms of multidimensional dynamics. However, for computational tractability, we consider here only reduced dimensionality dynamical models. The Appendix gives the appropriate definition of such a reduced dimensionality model in terms of two classes of internal coordinates; "active" coordinates $\mathbf{r}$ that are strongly involved in the reaction and "spectator" coordinates $\mathbf{Q}$ which are assumed to couple only weakly to the reaction coordinate. It is shown there that the role of the "spectator" coordinates should be included in the reduced dimensionality model by solving the $\mathbf{r}$ dynamics using an effective potential U_{eff}

$$U_{\text{eff}}(\mathbf{r}) = V_0(\mathbf{r}) + \frac{1}{2} \Sigma \hbar \omega_k(\mathbf{r}), \tag{2}$$

where $V_0(\mathbf{r})$ is the potential with all $\mathbf{Q}$ relaxed and $\omega_k(\mathbf{r})$ are the frequencies of the $\mathbf{Q}$ modes and which depend parametrically on $\mathbf{r}$.

For reduced dimensionality dynamical calculations, we need both the bare potential $V_0(\mathbf{r})$ and the "spectator" frequencies $\omega_k(\mathbf{r})$, for all $\mathbf{r}$. Often, only the bare PES $V_0(\mathbf{r})$ and frequencies of "spectator" modes at the transition state are calculated in the *ab initio* calculations. We therefore will assume that U_{eff} is identical in shape to the bare PES, but with the barrier height adjusted to contain the effects of "spectator" mode zero point.

For D_2 dissociation or associative desorption on Si(100), we take as "active" coordinates Z the distance of D_2 to the surface, D is the D_2 internuclear separation and a phonon coordinate Y. As "spectator" modes we take those modes which become the frustrated translations and rotations of the molecule–surface complex and which are not treated dynamically. Further, since the saddle point is the critical part of the PES defining reaction, we take the normal coordinates $\mathbf{Q}$ to be defined as those appropriate for the $\mathbf{r}$ corresponding to the transition state, i.e., the four modes and frequencies defined in Table I. Then, the barriers in the effective potential U_{eff} appropriate for D_2 dissociative adsorption are given as $\Delta U_{\text{asym}} = V^*_{\text{asym}} + 0.14$ eV for the asymmetric path and $\Delta U_{\text{sym}} = V^*_{\text{sym}} + 0.08$ eV for the symmetric path. V^*_X is the bare PES barrier and ΔU_X is the barrier on the effective potential U_X. Analogously, for desorption we find $\Delta U_{\text{asym}} = V^*_{\text{asym}} + \Delta H + 0.03$ eV and $\Delta U_{\text{sym}} = V^*_{\text{sym}} + \Delta H - 0.03$ eV where ΔH is the exothermicity of adsorption. All hindered external modes of the adsorbed monodeuteride phase are taken as 54 meV.[23] The differences in zero point corrections to the effective activation energies between adsorption and desorption simply reflect the differences in zero point of the adsorbed species relative to that of the gas phase species.

Once U_{eff} is available, only the relevant masses need be specified for full definition of the reduced dimensionality dynamical model. For D_2 on Si(100), we use obvious D_2 translational and vibrational masses for Z and D. For Y, we use a mass of 28 a.m.u. since this is the appropriate mass for rotation about the upper (largely fixed) Si atom of the dimer pair.

IV. *Ab initio* PES

In the D_2/Si(100) system, adsorption and desorption are intimately related to the reconstruction of the surface. At saturation coverage, no dangling bonds exist at the surface, and a reconstruction built up from flat, symmetric monodeuteride units is stable. On the clean surface, each atom of the Si dimers is associated with a dangling bond. Different reconstructions have been proposed for this surface. Meanwhile there is general agreement in the literature that the Si dimers are stabilized by buckling. This relaxation allows the lower Si atom to become closer to sp^2 hybridization, and the occupation of its dangling bond is reduced. The energetic gain from rehybridization is partly canceled by increased mechanical stress in the substrate. Several higher-order reconstructions, with $p(2 \times 2)$ or $c(4 \times 2)$ unit cells, have been proposed, that could possibly allow for a further stabilization of the buckled dimers on the clean surface. These reconstructions are locally undone by the adsorption of deuterium (or hydrogen). Upon adsorption of D_2, the lower Si atom of the dimer returns to sp^3 hybridization, and the extra surface stress associated with the buckling is released. The energetics of D_2 dissociation on Si(100) therefore involves a delicate interplay between the hybridization of the surface atoms and deformation of the substrate. *Ab initio* total-energy calculations give the opportunity to study this interplay in great detail.

The work presented here is mostly based on calculations employing a 2×1 surface unit cell, the smallest possible choice that allows for a correct description of the dimerization and buckling, and allowing for relaxation of two layers of the substrate. The technical details of the calculations are described in Ref. 23. Electronic exchange and correlation effects are accounted for within the framework of density functional theory, employing the gradient-corrected functional suggested by Perdew and co-workers.[25]

For a detailed dynamical study, a complete multidimensional PES is required. This poses a computationally difficult task, since the PES is a function of all molecular and substrate coordinates. To make the problem tractable, we use the 2×1 unit cell in the full PES calculations, and restrict ourselves to the most important molecular coordinates, Z and D as discussed in the previous section. Our aim is to develop a 3D PES for these two degrees of freedom and one substrate coordinate Y, and with all other coordinates in the unit cell fully relaxed. For both the symmetric and the asymmetric transition state, the following procedure was employed.

First we determine the PES in two molecular coordinates Z and D, freezing the impact site and molecular orientation to the geometry at the transition state and also freezing Y at the value yielding the lowest barrier. For the asymmetric transition state we assume that the molecule approaches (or leaves) the surface at an angle of ~60° from the surface normal, as suggested by the calculated forces acting on the molecule. For the symmetric transition state, approach per-

FIG. 2. Equipotential contours of the *ab initio* PES for D_2 interacting with Si(100) at a fixed phonon coordinate of $Y = -0.47$ Å. This produces contours about the asymmetric transition state in terms of the center of mass distance of the D_2 to the surface as measured by Z_0 and the D–D distance D. The contour interval is 0.05 eV and the origin of energy is given by the free surface ($Y = -0.69$ and Z_0 large) plus the energy of a free D_2.

pendicular to the surface is assumed. We have concentrated on the part of the PES around the transition state and between it and the gas-phase because this is the crucial part in determining both the dissociation probabilities and the amount of coupling between translation and surface vibration in desorption. Z vs D contour plots of the PES are shown in Figs. 2 and 3. They show the well-known elbow shape characteristic of a reactive PES. The asymmetric PES shows a more pronounced stretch of the D–D bond at the transition state.

The reaction path in the Z,D plane is determined from these contour plots by finding the steepest descent path from
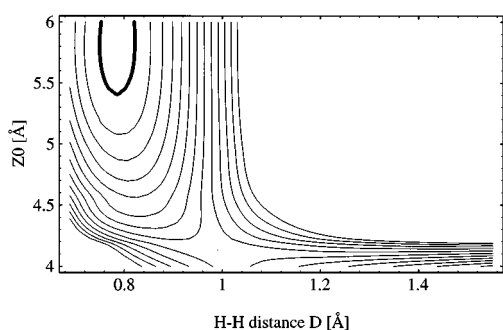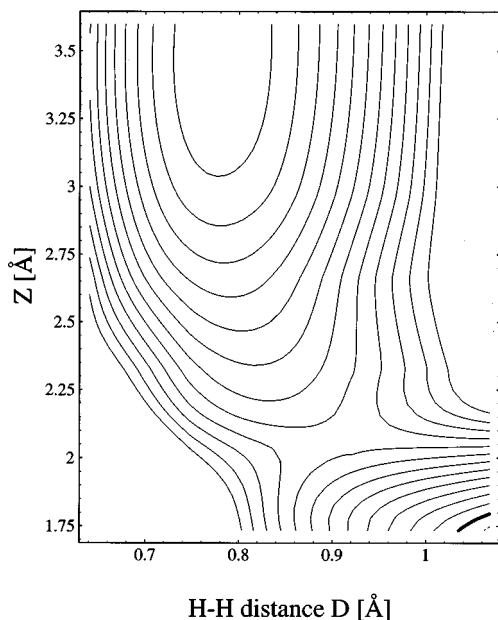

H-H distance D [Å]

FIG. 3. Equipotential contours of the *ab initio* PES for D_2 interacting with Si(100) at a fixed phonon coordinate of $Y = 0.$ Å. This produces contours about the symmetric transition state in terms of the center of mass distance of the D_2 to the surface as measured by Z and the D–D distance D. The contour interval is 0.05 eV and the origin of energy is given as the surface at $Y = 0$ (and Z large) plus the energy of a free D_2.

the transition state. In a second step, we calculate slices through the multidimensional PES for different values of Y, with the Z,D coordinates varying along the reaction path. In these calculations, the local geometry of the D–Si–D group in the asymmetric transition state (the local geometry of the Si–D–D–Si unit in the symmetric transition state) was held fixed when varying Y. [The potential energy for various Y (and for Z and D along the reaction path) is displayed in Figs. 5 and 7 for the asymmetric and the symmetric paths respectively. This procedure allows us to sample the relevant information contained in the 3d PES of Z,D,Y coordinates and insures that the forces about the minimum energy path are correct.]

To check the validity of these results, we also perform some calculations using a $c(4\times2)$ unit cell. The two Si dimers in this unit cell were both allowed to relax freely, and a ground state with alternating buckling is determined for the bare surface. Substrate relaxation was taken into account in the first four layers of Si to allow for a better convergence of the elastic energy contribution. D_2 is placed above one of the Si dimers, in the local geometry of either the asymmetric or the symmetric transition states determined via the (2×1) unit cell, and again the substrate is allowed to relax. The barrier height in the $c(4\times2)$ unit cell is calculated using the true $c(4\times2)$ ground state, with alternating buckling, as the reference for the potential energy. For the asymmetric transition state, we recover the result that the Si dimer active in the reaction is less buckled than the bare surface. The Si dimer not involved in the reaction, on the other hand, shows a slightly stronger buckling than the bare surface equilibrium. This larger calculation results in a value for the barrier height of 0.24 eV, slightly lower than the 0.48 eV obtained with the 2×1 unit cell. The difference might be due to the fact that elastic strain can be relaxed more easily if more degrees of freedom in the Si substrate are included. For the symmetric transition state, we considered both configurations where the neighboring, inactive Si dimer was either buckled or horizontal. The reaction barrier was found to be 0.59 eV in both cases, in close agreement with the 0.56 eV obtained using the 2×1 unit cell. We conclude that the calculations using the 2×1 unit cell give a correct qualitative picture of the PES governing the reaction, but that the value for the barrier height for the asymmetric transition state is slightly lower than inferred from these smaller calculations.

V. MODELS OF U_{eff}

Simple analytic forms are needed to model U_{eff} [Eq. (2)] for use in the dynamical calculations and which are based on the *ab initio* PESs described in the previous section. The general procedure will be to assume that the shapes of U_{eff} are similar to those of the *ab initio* bare PES from the (1×2) unit cell calculations, but that barrier heights ΔU_X are based on the *ab initio* $c(4\times2)$ V_X^* and zero point corrections (vibrational frequencies at the transition state) are obtained from the (1×2) calculations. These model U_{eff} PES assume that the total PES is divided into two regions; an entrance

channel described by a molecular potential V_M and an exit channel described by an atomic potential V_A. The total PES is given via a Lennard-Jones style mixture,

$$U_{eff}(Z,D,Y) = 0.5[V_A + V_M - \sqrt{(V_A - V_M)^2 + \chi^2}], \quad (3)$$

where χ is a mixing parameter.

A. Asymmetric U_{eff}

In this section, we present the model PES for the asymmetric reaction path. In this case, V_M is given as

$$V_M = W_m F_m[F_m - \gamma_m(Z_D)] - V_{min}(Z_D)$$
$$+ 0.5\kappa(Y + 0.69)^2 + V_m e^{-\alpha_m(Y)Z_D}. \quad (4)$$

The appropriate distance parameter to the surface Z_D is taken as the perpendicular distance of the D_2 center of mass to the lower Si atom in the dimer pair, $Z_D = \cos(60°)(Z_0 - Y)$ with Z_0 the oblique coordinate corresponding to the $\sim 60°$ approach to the surface. The origin of the phonon coordinate Y is taken as the flat dimer and spans the range 0 to -0.75 Å.

The first two terms describe a Morse-like potential between the two D atoms in D_2. However, the well depth is weakened and the equilibrium bond length stretched in a smooth fashion as the molecule approaches the surface. This form of a modified Morse potential has been defined previously;[26] W_m is the free D_2 well depth, $F_m = e^{-\lambda_m(D - D_0)}$ the exponential term in the free D_2 Morse potential, $\gamma_m(Z_D)$ is a variable attraction term and is given as $\gamma_m(Z_D) = (2 - \eta_m) + \eta_m \tanh[(Z_D - O_Z)/W_Z]$ and $V_{min}(Z_D)$ is the Z_D dependent well depth of the D_2 molecule. Parameters for the free molecular Morse potential were typical D_2 parameters. The third term in Eq. (4) represents the potential of the dimer phonon. Since this PES was originally intended to only describe dissociative chemisorption, and Y is only modestly changed at the transition state from that of the free surface, we have used a harmonic approximation (centered about the free surface buckling). κ is chosen to give a surface phonon frequency of 20 meV, close to that in the *ab initio* calculations.[23] The last term describes the Pauli repulsion as D_2 approaches the surface. In order to force the minimum barrier to occur for $Y = -0.47$ Å, the exponential term is made a function of Y, $\alpha_m(Y) = \alpha_m + 0.15 e^{-(Y + 0.47)^2/0.0625}$.

In a somewhat similar manner, V_A was defined as

$$V_A = 2W_a F_a[F_a - \gamma_a(D)] - V_{min}(D) + 0.5\kappa Y^2$$
$$+ V_\alpha e^{-\alpha_a D}. \quad (5)$$

The first two terms describe a Morse like potential between a D atom and the surface (lower Si atom of the dimer pair). However, as before the well depth is weakened and the equilibrium bond length stretched in a smooth fashion as the D atoms come together to form a molecule. This describes the fact that the atoms cannot make bonds to the surface until the intermolecular bond is broken. W_a is the D–Si well depth, $F_a = e^{-\lambda_a(Z_D - Z_0)}$ the exponential term in the bare D–Si Morse potential, $\gamma_a(D)$ is the variable attraction term and is given as $\gamma_a(D) = (2 - \eta_a) + \eta_a \tanh[(D - O_D)/W_D]$ and $V_{min}(D)$ is the D-dependent well depth of D–Si. W_a,

TABLE II. Potential energy parameters used in the model PES.

PES parameter	Asymmetric PES	Symmetric PES
W_m (eV)	4.75	4.75
λ_m (Å^{-1})	1.95	1.95
D_0 (Å)	0.74	0.74
η_m	0.5	0.15
O_Z (Å)	1.85	1.91
W_Z (Å)	0.26	0.26
κ (eV Å^{-2})	2.71	2.71
V_m (eV)	350.	150.
α_m (Å^{-1})	3.07	2.55
W_Y (eV)	...	0.14
λ_Y (Å^{-1})	...	3.10
W_a (eV)	3.57	3.57
λ_a (Å^{-1})	1.46	1.46
Z_0 (Å)	1.53	1.53
η_a	0.5	0.5
O_D (Å)	1.06	0.87
W_D (Å)	0.26	0.26
V_a (eV)	20.	17.5
α_a (Å^{-1})	1.89	2.08
χ (eV)	1.0	1.0

λ_a, and Z_0 are taken to match typical D–Si bond energies, vibrational frequencies, and equilibrium lengths. The second and third terms are the harmonic phonon potential and an exponentially repulsive term to force the dissociated atoms apart. The same phonon force constant is used here as in V_M. Parameters used in the model PES are given in Table II.

The top part of Fig. 4 shows Z_0 vs D contours of this model PES for a fixed value of $Y = -0.47$ Å which corresponds to the Y of the minimum barrier. This barrier is 0.47 eV, slightly in excess of the barrier in the effective potential U_{asym} of 0.38 eV [based on the c (4×2) supercell]. We also see that the D–D bond is stretched nearly 0.22 Å at the transition state, in very good agreement with the *ab initio* PES (see Fig. 2).

The bottom part of Fig. 4 shows Z_0 vs Y contours of the model PES. D values were adjusted for each Z to fall along the path of steepest descent in the Z_0 vs D contours of the top part of the figure (D_{sd}). This contour plot illustrates the shift in the minimum energy with Y as D_2 approaches the surface. It also shows that the contours are rather flat along Y in the region of the entrance channel likely to be important in dissociation (or desorption) dynamics.

Figure 5 compares one dimensional cuts through the model U_{asym} PES to similar cuts through the *ab initio* PES based on the (1×2) supercell calculations. These cuts are plotted as a function of Z_0 for fixed Y and for D chosen as D_{sd}. It is evident that there is very good qualitative agreement between the model and *ab initio* PES. The variation of the barrier height with Y is similar as well as the fact that the barrier moves in and out along Z_0 as a function of Y. To anticipate dynamical calculations, we note that the variation of barrier height with Y and the breathing in and out of the barrier with Y (so-called "recoil") can both produce a dynamic coupling to the phonon coordinate.
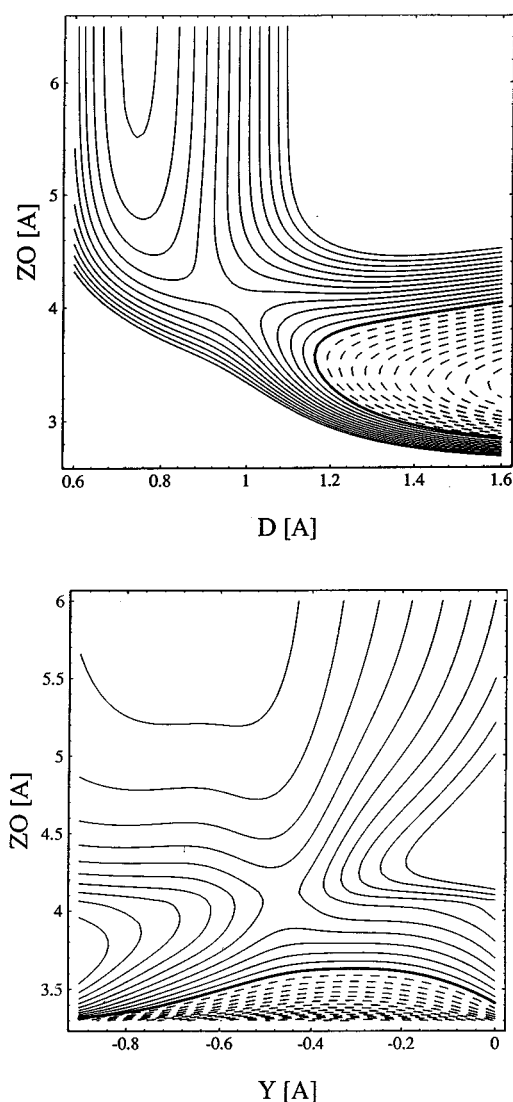
FIG. 4. Equipotential contours of the model U_{asym} PES about the asymmetric path. Contour intervals are 0.1 eV. The thickest contour represents the zero of energy, solid lines are positive energy contours and dashed lines are negative energy contours. The zero of energy is taken for Z_0 large and $Y = -0.69$ Å. (top) Contours plotted as a function of the oblique distance to the surface Z_0 and internuclear separation D for a fixed $Y = -0.47$ Å. (bottom) Contours plotted as a function of the oblique distance to the surface Z_0 and the phonon coordinate Y. D is chosen for each Z_0 as that of steepest descent from the transition state at $Y = -0.47$ Å.

FIG. 5. Comparison of the model U_{asym} to the *ab initio* PES in the general region of the asymmetric transition state. Several one-dimensional "cuts" through the PES are presented at different Y. The potential energy $V(Z_0, D_{sd}, Y)$ is plotted against Z_0. D_{sd} is the value of D obtained at each Z_0 by steepest descent on the PES at a fixed $Y = -0.47$ Å. (a) *ab initio* PES and (b) model U_{asym}.

B. Symmetric U_{eff}

The model U_{sym} PES about the symmetric path was created in a similar manner to that for the asymmetric one. V_M is given as

$$V_M = W_m F_m [F_m - \gamma_m(Z_D)] - V_{min}(Z_D) + W_Y F_Y (F_Y - 2)$$
$$+ V_m e^{-\alpha_m Z_D}. \tag{6}$$

The appropriate distance parameter to the surface Z_D in this case is taken as $Z_D = Z - 0.4Y$ with Z as the normal distance of D_2 to the flat dimer. Because V_M samples a very wide range of Y from the asymptotic entrance channel to the transition state in this case, it was not sufficient to use a har-
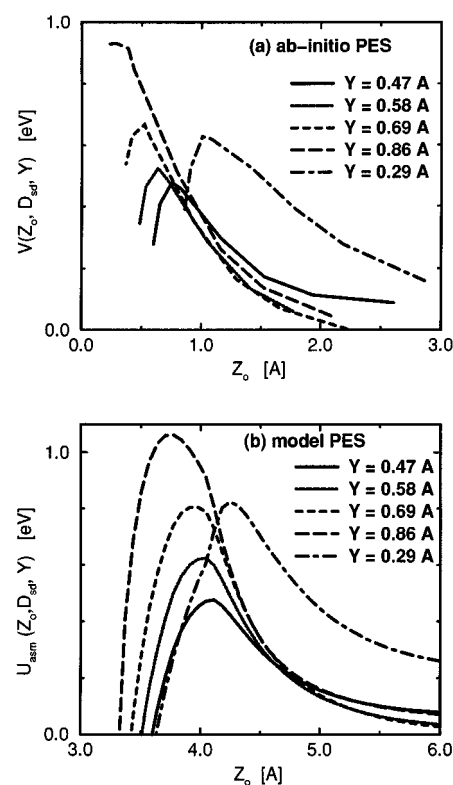
monic approximation for the phonon coordinate. We utilized a Morse potential in $-|Y|$ centered at $Y = 0.69$ Å, e.g., $F_Y = e^{-\lambda_Y(-|Y| + 0.69)}$. Also, in this case it was not necessary to make the Pauli repulsion term Y dependent to force the minimum barrier to the flat dimer position. V_A was the same as that in Eq. (5). For this part of the PES, a harmonic approximation to the phonon coordinate was appropriate. The parameters for this PES are also given in Table II.

The top half of Fig. 6 gives the Z vs D potential contours for this model PES and for $Y = 0$. The overall barrier height relative to the entrance channel is ca. 0.65 eV, in very good agreement with the barrier of 0.67 eV for U_{symm} based on the *ab initio* calculations [and the $c(4 \times 2)$ supercell for bare PES barrier height]. At the transition state along this path, the D–D bond is stretched ca. 0.1 Å, considerably less than in the transition state for the asymmetric path. This contour diagram is also in very good agreement with the *ab initio* bare PES of Fig. 3.

The bottom part of Fig. 6 shows Z vs Y contours of the model PES for values of D as D_{sd} from the top part of the figure. This plot illustrates how the minimum in energy varies from $|Y| = 0.69$ Å to $Y = 0$ as the D_2 approaches the surface and dissociates. A barrier increase with Y is also evident.

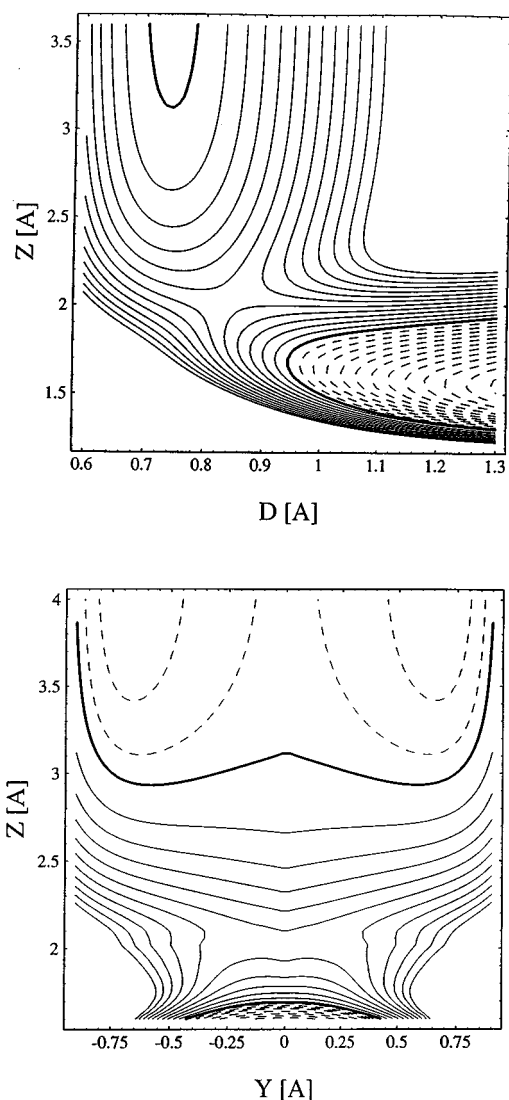Figure 7 compares one dimensional cuts through this

FIG. 6. Equipotential contours of the model U_{sym} about the symmetric path. The thickest contour represents the zero of energy, solid lines are positive energy contours and dashed lines are negative energy contours. Positive contour intervals are 0.1 eV and negative contour intervals 0.05 eV. The zero of energy is taken for Z large and $Y = 0$ Å. (top) Contours plotted as a function of the distance to the surface Z and internuclear separation D for a fixed $Y = 0$ Å. (bottom) Contours plotted as a function of the distance to the surface Z and the phonon coordinate Y. D is chosen for each Z as that of steepest descent from the transition state at $Y = 0$.
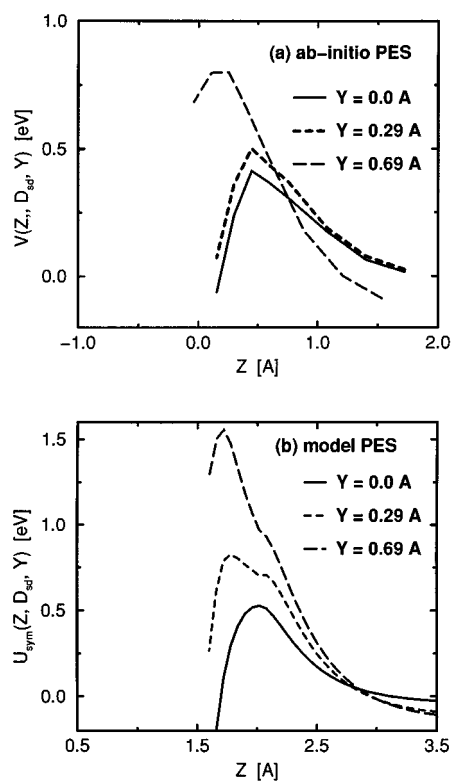

FIG. 7. Comparison of the model U_{sym} to the *ab initio* "bare" PES in the general region of the symmetric transition state. Several one-dimensional "cuts" through the PES are presented at different Y. The potential energy $V(Z, D_{\text{sd}}, Y)$ is plotted against Z. D_{sd} is the value of D obtained at each Z by steepest descent on the PES at a fixed $Y = 0$. (a) *ab initio* PES and (b) model U_{sym}.

model PES to those for the *ab initio* PES. These cuts are plotted as a function of Z for fixed Y and for D_{sd} at the given Z. Although there is good qualitative agreement between these two, the model PES contains a somewhat stronger variation of the barrier height with Y. However, it must be remembered that the model is a model of U_{sym} and not the bare *ab initio* PES. Again, to anticipate dynamical calculations, we note that for the symmetric path, there is very little breathing in and out of the barrier with Y, i.e., little "recoil."

VI. DISSOCIATIVE ADSORPTION

Because tunneling has been suggested to be important in the dynamics and as a possible resolution of the dissociation–desorption paradox, we have utilized conventional wavepacket quantum dynamics to solve for dissociation on the reduced dimensionality ($3d$) model PES of U_X described in the previous section. The dependence of the dissociation probability S on incident energy E_i is calculated for initial D_2 vibrational states v and initial surface oscillator states n. The T_s dependence is calculated for $v = 0$ states at several fixed E_i by performing Boltzmann averages over separate calculations for a range of initial n. The details of such calculations are similar to those described previously for the dissociation of alkanes on metal surfaces.[27]

A. Asymmetric path

1. Dependence of S on E_i

The top portion of Fig. 8 shows the logarithm of the calculated dissociation probability for D_2 on Si(100) as a function of E_i for both $v = 0$ and $v = 1$ with $n = 0$ ($T_s = 0$). S for $v = 0$ and $n = 0$ is also shown using a simple "sudden" dynamical calculation based on the same PES (see below).

For $v = 0$, where the most extensive calculations exist, the dependence on E_i can be approximately divided into two regions. Below an energy of ~ 0.45 eV, S is dominated by tunneling and decreases exponentially with decreasing E_i. Above this energy, S increases only slowly with increasing
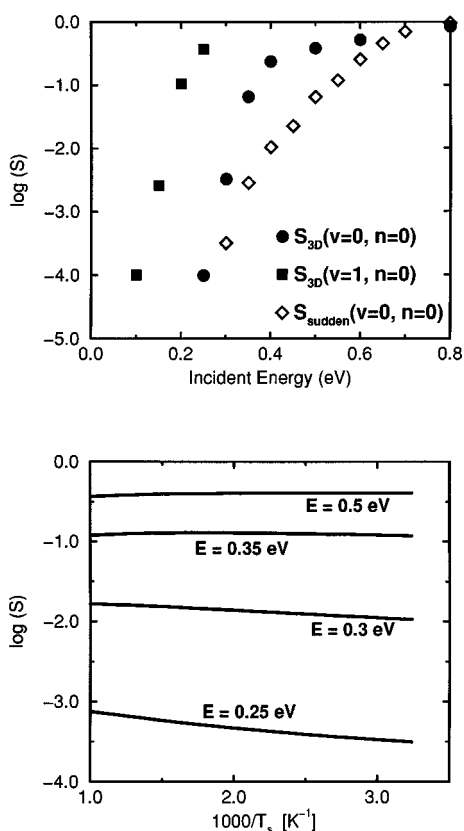
FIG. 8. Quantum dynamical calculation of the dissociative chemisorption probability S using U_{asym} as the PES log (S) is plotted as a function of initial energy for different initial D_2 vibrational states v and for $T_s = 0$ ($n = 0$) (top) and as a function of reciprocal surface temperature for different incident energies E (bottom). A sudden calculation of S is also given for comparison in the top part of the figure.

E_i. In this region, the rather gradual approach to the asymptotic high energy limit ($S = 1$) is due to energy transfer into the lattice so that not all of E_i is available to reaction. Note that the boundary between the two regions appears to be approximately at the barrier along the minimum energy path ($Y = -0.47$ Å), rather than at 0.8 eV, the barrier in the model potential at the initial dimer tilt angle ($Y = -0.69$ Å). This suggests that there is considerable "steering" of the Y coordinate as the D_2 approaches the surface, especially at low E_i. This contention was confirmed by looking at the actual coordinate dependences of the wave packets during the time evolution of the system. As the D_2 approached the surface, there is almost complete steering in Y before hard impact with the surface.

Further confirmation for the importance of steering is evident in a comparison with the results of a sudden calculation based on the same PES. S_{sudden} is given by

$$S_{sudden}(v=0, n=0) = \int S_{2d}(Z,D;Y)|\psi_0^*(Y)\psi_0(Y)|dY,$$
(7)

with $S_{2d}(Z,D;Y)$ the results of a two-dimensional dynamical calculation based on a fixed value of Y for the surface oscil-

lator coordinate in the model PES and $\psi_0(Y)$ the ground state vibrational eigenfunction for the surface oscillator. This sudden approximation neglects all dynamic coupling to the Y coordinate, i.e., both "steering" and energy transfer to the lattice ("recoil"). Over most of the energy range, $S_{sudden}(v=0, n=0)$ is nearly two orders of magnitude less than the full three-dimensional dynamical calculation $S_{3d}(v=0, n=0)$. This difference reflects the importance of "steering" in finding the minimum energy path. At the highest E_i, $S_{sudden}(v=0, n=0)$ is in fact larger than $S_{3d}(v=0, n=0)$, reflecting the neglect of energy transfer to the lattice in the sudden approximation.

Several previous qualitative discussions of the dissociation of H_2 and D_2 on Si(100)[10,11,15] have been based on the sudden approximation. We see here that such an approximation is not particularly valid. The justification cited for the applicability of the sudden approximation was a time scale argument, i.e., that the vibrational period of a surface atom is an order of magnitude longer than the collision time. However, the sudden approximation is formally based on a semiclassical approximation and the assumption that $\tau_c \omega_{if}/\hbar \approx 0$, where τ_c is the collision time and ω_{if} is the frequency difference between the initial and final states. Hence, the sudden approximation also depends on the extent of energy transfer as well. The wavepacket calculations show modest energy transfer to the surface ($\Delta n > 1$) at impact (principally due to recoil). Thus, the limited separation of the time scales coupled with the energy transfer do not make the sudden approximation a very accurate description of the full dynamics.

The shift of the curve for $S_{3d}(v=1, n=0)$ towards lower E_i relative to that of $S_{3d}(v=0, n=0)$ is in complete accord with expectations based on the Z vs D contour plot (top of Fig. 4). Many two-(and higher) dimensional dynamic studies[28] have emphasized the role of initial vibration as well as translation in overcoming a barrier when the saddle point occurs at a stretched vibrational coordinate D. For this system, a so called vibrational efficacy of ~ 0.5 is obtained for D_2, i.e., the shift of the sticking curve to lower E_i is roughly half of the added vibrational energy.

2. Dependence of S on T_s

The lower part of Fig. 8 shows the calculated T_s dependence for $S_{3d}(v=0)$ plotted in an Arrhenius fashion for several initial incident energies. The T_s dependence is very small and only mildly dependent on initial energy. To the extent that the T_s dependence can be phenomenologically described by an Arrhenius expression, the apparent activation energy at $E_i = 0.25$ eV is only 0.04 eV. It must be emphasized, however, that the T_s dependence in this calculation arises from purely dynamic coupling and the Arrhenius expression and apparent activation energy have no fundamental meaning.

The weakness of the T_s dependence of S implies that the net dynamic coupling of the reaction to the lattice is rather weak. This conclusion is also qualitatively suggested in the Z_0 vs Y potential contour (bottom of Fig. 4) since the poten-

tial energy in the entrance channel is relatively independent of Y over most of the PES region sampled prior to dissociation. As discussed previously in Sec. V A and exemplified in Figs. 1 and 5, there are two types of dynamic couplings for the asymmetric path. First, as the D_2 approaches Si(100), the D_2 "pulls" on the lower Si atom of the dimer pair in an attempt to decrease $|Y|$ and minimize the barrier to dissociation. However, in addition, the incoming D_2 "pushes" on the repulsive wall of the lower Si atom, i.e., couples via "recoil." The full dynamic coupling is the sum of both effects, and since they oppose each other the net coupling is quite weak. This cancellation can be quantified by comparing the forces $\partial V(Z,D,Y)/\partial Y$ along the reaction path for the model PES in which the full coupling is present to others in which "recoil" is explicitly excluded or where only "recoil" coupling is included. Over most of the entrance channel, the forces due to recoil dominate. The net forces, however, are considerably smaller than for a PES where either coupling alone is present. Dynamic calculations where only recoil is present in the model PES predict a T_s dependence of S many order of magnitudes larger than that in Fig. 8.

Another recent quantum dynamical calculation,[29] similar in spirit to that presented here, finds substantially larger T_s dependence. This calculation, however, is based on a different model of the *ab initio* PES than that used in this paper. In particular, their model PES, while accounting for the modulation of the barrier up and down with Y contains very little "recoil," i.e., modulation of the barrier in and out with Y, and which is clearly apparent in the *ab initio* points. We suspect that this accounts for their finding of a much larger dependence of S_0 on T_s since the two modulations oppose each other. There must remain, however, some uncertainty in the magnitude of the T_s effects since the net coupling is caused by the cancellation of two larger couplings.

B. Symmetric path

1. Dependence of S on E_i

The top portion of Fig. 9 shows the logarithm of the calculated dissociation probability for D_2 on Si(100) as a function of E_i for $v=0$ and $n=0$ ($T_s=0$) on the model PES about the symmetric path. Below $E_i \approx 0.8$ eV, the dissociation probability decreases roughly exponentially with decreasing E_i. At an $E_i=0.65$ eV corresponding to the barrier height along the minimum energy path ($Y=0$), the dissociation probability is still relatively small. This low probability implies that "steering" to the minimum energy configuration is not as dominant on this PES. Instead, the dissociation process seems to proceed with barriers characteristic of a range of Y intermediate between $Y=0$ and the initial state $Y=-0.69$ Å (see Figs. 6 and 7).

2. Dependence of S on T_s

The bottom part of Fig. 9 shows the calculated dependence on T_s for several initial E_i (for $v=0$). In terms of a phenomenological Arrhenius expression, the results can be approximately described in terms of apparent activation en-
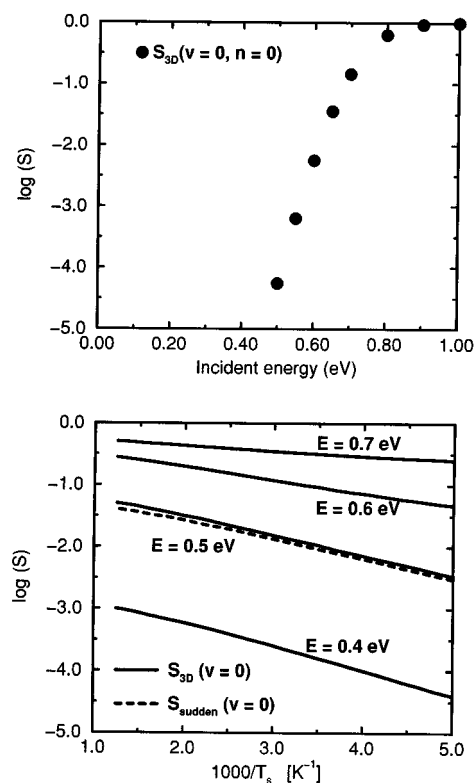

FIG. 9. Quantum dynamical calculations of the dissociative chemisorption probability S using the model PES U_{sym} log (S) is plotted as a function of initial energy for the ground D_2 initial state and for $T_s=0$ ($n=0$) (top) and as a function of reciprocal surface temperature for different incident energies E (bottom). A sudden calculation of S at $E=0.5$ eV is also given for comparison in the bottom part of the figure.

ergies; 0.07 eV at $E_i=0.4$ eV decreasing to 0.02 eV at $E_i=0.7$ eV. Again, such Arrhenius expressions have no fundamental meaning.

This T_s dependence is also quite weak. Inspection of the contours at the bottom of Fig. 6 shows that the potential is nearly independent of Y over much of the entrance channel (excepting the actual barrier and far entrance channel region), again indicative of weak dynamic coupling. We also compare the T_s dependence calculated dynamically to that predicted using a sudden approximation for $E_i=0.5$ eV.

$$S_{\text{sudden}}(v=0,T_s)$$

$$= \int \sum_n P_n S_{2d}(Z,D;Y) |\psi_n^*(Y)\psi_n(Y)| dY, \quad (8)$$

with $S_{2d}(Z,D;Y)$ the results of a two dimensional dynamical calculation based on a constant value of Y for the surface oscillator coordinate in the model PES, $\psi_n(Y)$ the nth state vibrational eigenfunction for the surface oscillator and P_n is the relative Boltzmann population of the nth surface oscillator state at T_s. In the sudden approximation, an increase in S with T_s should arise from anharmonicity in the surface oscillator (when D_2 is far from the surface) since the higher the excitation of n, the smaller is the centroid of $|Y|$ and the lower the barrier to dissociation (see Z vs Y contours in Fig.
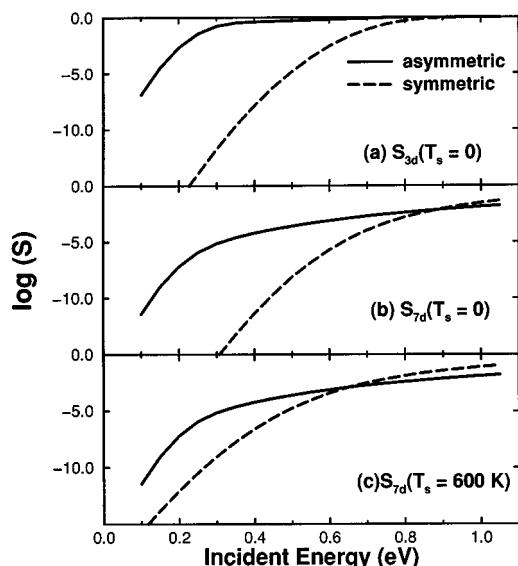
FIG. 10. Comparison of the dissociative chemisorption probability through the asymmetric (solid line) and symmetric (dashed line) paths. The results for both are based on best estimates of the barrier heights of U_{eff}. (a) $S_{3d}(T_s=0)$, (b) $S_{7D}(T_s=0)$, and (c) $S_{7D}(T_s=600 \text{ K})$.

6). The result (dashed line in the bottom of Fig. 9) is nearly indistinguishable from the full dynamic calculations. Thus, the T_s dependence in the dynamic calculations is nearly fully determined by the static initial state properties. In this case, energy transfer to the lattice is even smaller than in the asymmetric case due to the smaller "recoil." Hence, the sudden approximation appears to be more valid.

C. Comparison of asymmetric and symmetric paths

For a comparison of the relative importance of the asymmetric and the symmetric paths in dissociative chemisorption, it is important that the best estimates of the PES barriers in U_{eff} be utilized. Based on the barrier height calculations from the $c(4 \times 2)$ supercell, combined with the vibrational frequencies of the **Q** modes from the (1×2) supercell (Table I), we estimate barrier heights of 0.38 and 0.67 eV for the asymmetric and symmetric paths, respectively. These barriers are slightly different than those of the model PES used in the calculations for Figs. 8 and 9. We therefore use the static approximation outlined in the Appendix [Eq. (A13)] to adjust the calculations of Figs. 8 and 9 to those appropriate for the best estimate barriers. Results for $v=0$ and $n=0$ ($T_s=0$) using this correction are shown in Fig. 10(a). It is evident that because of the lower barrier, the asymmetric path is predicted to dominate all sticking measurements. This comparison, however, neglects entirely the importance of the vibrational phase space associated with the "spectator" modes.

Figure 10(b) shows the predicted $7d$ dissociation dynamics when the external **Q** coordinates (Table I) are included via the static approximations outlined in Eq. (A14) of the Appendix. For the plot, we have somewhat arbitrarily chosen a value of $\xi=0.2$. This corresponds to moderate steering. We note the large decrease in S for both dissociation

paths, even at very large E_i. This reduction of S is due to the restricted vibrational phase space for dissociation caused by the relatively large vibrational frequencies of the external modes at the transition state. These curves include all aspects of the so called "entropic" barriers discussed by Kolasinski et al.[15] The suppression of S for the asymmetric path is larger than for the symmetric path, in complete agreement with the phase space estimates of transition state theory (Sec. II). The rationale for the smaller phase space of the asymmetric path is again the higher frequencies of the frustrated translations at the transition states. We now see that inclusion of the phase space produces a dominance of the symmetric path for incident energies above 0.8 eV. Smaller values of ξ produce even larger reductions in S and lower incident energies for the crossover between asymmetric and symmetric dominated dissociation.

Because S increases with T_s more for the symmetric path than the asymmetric one, the symmetric path becomes increasingly important as T_s is raised. Figure 10(c) shows the predicted dissociation probabilities for $7d$ dynamics and for a $T_s=600$ K, again with $\xi=0.2$. We see that the symmetric path is predicted to dominate at this T_s for all $E_i > 0.6$ eV.

Averaging the $7d$ sticking curves of Fig. 10 over a thermal distribution of E_i characteristic of a gas temperature $T_g=300$ K yields thermally averaged sticking coefficients. Because of the uncertainty of the extent of steering and the approximations inherent in the multidimensional formulation, we make no conclusions about the absolute magnitude of the thermal S. For $T_s=600$ K, contributions to the thermal ($T_g=300$ K) S are now only two orders of magnitude larger from the asymmetric than the symmetric path. When $T_g=T_s \sim 750$ K, the contributions are equivalent from both paths. Note that this is the same conclusion as reached via the TST arguments. In the convolutions, incident energies of ca. 0.3–0.4 and 0.5–0.6 eV dominate the thermal S for the asymmetric and symmetric paths respectively, depending upon T_g. This demonstrates that classical "over the barrier" dissociation is a reasonable description of the thermal rates, and tunneling effects seem to be rather minor in dissociation.

VII. ASSOCIATIVE DESORPTION

The simplest possible dynamical model to describe associative desorption involves solving the same dynamics as for dissociation, but backwards. We take initial conditions for the wavepackets (or classical trajectories) as those appropriate for two adsorbed D atoms on the surface that are well separated. In this entrance channel for desorption, motion along Z is initial vibration of the D–D pair against the surface (quantum state v_z) while motion along D is represented as the two atoms approaching each other with initial translational energy E_D. For quantum dynamics, this latter is represented as a Gaussian wave packet. Y is defined identically as in dissociation. The exit channel for desorption corresponds to the D_2 leaving the surface with vibrational state v and with translational energy E_f. Just as in dissociation, we consider that only these three modes are "active" and couple to the reaction coordinate. All other modes are considered as
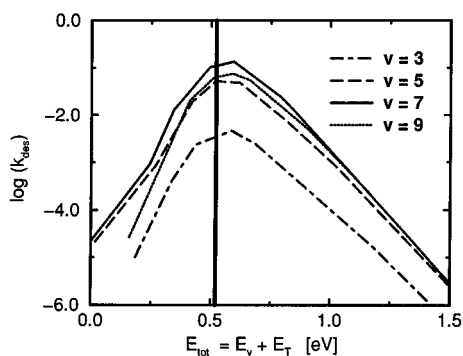
FIG. 11. Quantum two dimensional dynamical calculations of associative desorption of D_2 from Si(100) through the symmetric path. k_{des} is the relative desorption rate for a given initially adsorbed state v_z and for initial relative energy E_D. k_{des} depends both on the desorption probability and the Boltzmann population of the initial state. Results are plotted against the total energy E_{tot}. The dark vertical line marks the location of the classical barrier (relative to the same origin as in Fig. 6).

"spectators." In this model of desorption, we assume that all energy transfer between the "spectator" modes and the "active" modes occurs in the entrance channel, so that desorption can be viewed as an initial value problem. The population of all initial states and energies is assumed to be Boltzmann at the surface temperature T_s. Alternatively, it is possible to consider desorption models where most of the energy transfer between "spectator" and "active" modes occurs near the transition state and a Boltzmann distribution of states there and along the reaction coordinate are the initial conditions.[30] Since our interest in desorption is principally in the extent of energy transfer from translation to the lattice in the desorption exit channel, and this is essentially the same in the two models, we treat only the entrance channel model in reduced dimensionality dynamics.

To assess the importance of tunneling in the desorption process, we first consider a two-dimensional quantum dynamical model for desorption through the symmetric transition state. We calculate (relative) desorption rates k_{des} $= P_{v_z} P_{E_D} S_{des}(v_z, E_D)$, where P_{v_z} and P_{E_D} are Boltzmann populations of the initial states v_z and E_D at T_s and $S_{des}(v_z, E_D)$ is the dynamic calculation for desorption obtained by solving the sticking problem backwards with the initial conditions v_z and E_D. k_{des} for $T_s = 750$ K is shown in Fig. 11 for several initial v_z and plotted against the total energy $E_{tot} = E_{v_z} + E_D$. Initial excitation in both v_z and E_D are necessary for a large $S_{des}(v_z, E_D)$. This is consistent with the PES topology evident in the Z vs D contour at the top of Fig. 6. The heavy vertical line in Fig. 11 indicates the classical barrier position for U_{sym}. k_{des} peaks near this barrier. The decreases at E_{tot} below the barrier is due to fall off of $S_{des}(v_z, E_D)$ due to tunneling, while the decrease above the barrier is due to the fall off of the Boltzmann populations of the initial states. Again, this is the traditional picture of a classical reaction, i.e., where the overall reaction is dominated by the tail of the Boltzmann distribution of initial states at the top of the barrier. We thus conclude that the

early suggestion[18] that tunneling could account for the discrepancy between adsorption and desorption barriers cannot be valid. Because tunneling does not seem to dominate desorption, we employ a quasiclassical treatment for the model where coupling to Y is included dynamically.

Quasiclassical three dimensional dynamical models of desorption consisted of solving the classical equations of motion (trajectories) on the model PES of U_{eff} using quasiclassical initial conditions for the surface oscillator state n, the vibration against the surface v_z and for translation E_D. For the vibrations, these involved using the quantum energy levels as initial energies and an average over vibrational phase. All initial states were taken from Boltzmann distributions for a $T_s = 750$ K. Metropolis Monte Carlo averaging of many trajectories (typically 50 000) was used to obtain all average properties of thermal desorption. Importance sampling was used to only sample total energies $E_{tot} = E_D + E_{v_z} + E_y$ above ΔU_{eff}–0.1 eV since all total energies below the barrier cannot desorb classically.

Desorption on the symmetric PES predicts the following classical averages for the three final energies; $\langle E_f \rangle = 0.63$ eV, $\langle E_v \rangle = 0.11$ eV and $\langle E_y \rangle = 0.10$ eV. The most important finding is that the particle desorbs with substantial translational energy E_f. In fact, the amount of energy lost to the lattice $\langle \delta E_y \rangle$ is only 0.05 eV. This result is quite consistent with the weak T_s dependence calculated in sticking and the conclusion that there is only weak dynamic coupling. It is, however, inconsistent with models based on *ad hoc* PES which assume large coupling to the lattice and hence energy loss to the lattice upon desorption.[21]

By binning final vibrational states, we find $P_{v=1} = 0.17$. We anticipate, however, that $P_{v=1}$ is overestimated in the entrance channel model of desorption due to the "bobsled" effect in which trajectories overshoot after passing the barrier. Desorption models starting at the transition state should provide a better estimate for this probability.

The total energy available to the system in desorption is $\langle \Delta U_{sym} \rangle + 3k_B T_s$, where $\langle \Delta U_{sym} \rangle$ is the average barrier seen in desorption. Comparison with the observed final energies shows that $\langle \Delta U_{sym} \rangle \approx 0.65$ eV, the minimum barrier on U_{sym}. Thus, the entrance channel model of desorption is consistent with the fact that the minimum barrier dominates desorption, as assumed in transition state desorption models.

Desorption from the asymmetric PES predicts the following averages for the three final energies; $\langle E_f \rangle = 0.45$ eV, $\langle E_v \rangle = 0.15$ eV and $\langle E_y \rangle = 0.04$ eV. Again, the D_2 desorbs with substantial translational energy E_f and $\langle \delta E_y \rangle \approx 0$. The result for this PES is also inconsistent with models assuming large energy loss to the lattice. In this case $P_{v=1} = 0.33$, again probably overestimated by the "bobsled" effect. The larger $P_{v=1}$ here relative to that from the symmetric path is consistent with the two PES topologies evident in the Z vs D contours (Figs. 4 and 7). The total energy available here for desorption is $\langle V_{asym}^* \rangle + 3k_B T_s$. Comparison with the observed final energies shows that $\langle V_{asym}^* \rangle \approx 0.47$ eV, the minimum barrier on U_{asym}, as assumed in transition state models.

As outlined in Sec. II and the Appendix, the relative

importance of multidimensional desorption through the two transition states is well approximated via transition state theory. Both are predicted to contribute approximately equally in thermal desorption since phase space considerations largely offset the lower barrier of U_{asym} relative to U_{sym}.

VIII. DYNAMICAL MODEL CONTRA EXPERIMENT

A. Adsorption

There have been two reported measurements of dissociative adsorption of D_2 on Si(100). Molecular beam experiments by Kolasinski et al.[15] observed values of $S \approx 10^{-5}$, a weak increase in S with incident energy (0.08 to 0.35 eV) and a weak increase in S with T_s (300 to 650 K) for low incident E_i. Höfer and co-workers[19,20] have measured the T_s dependence of S over a wide range of temperatures for thermal ($T_g = 300$ K) gas adsorption. They find an extremely strong Arrhenius increase in S with T_s with an apparent activation energy of ca. 0.7 eV. At $T_s = 550$ K, $S \approx 10^{-8}$, increasing to $\approx 10^{-5}$ at $T_s = 1000$ K. These results are qualitatively similar to their previous results on Si(111).[17] Thus, although the conditions of the two experiments are somewhat different so that an exact comparison is impossible, the two are nevertheless in considerable qualitative disagreement. Magnitudes of S observed by Kolasinski et al. are orders of magnitude larger than those of Höfer and co-workers (at low T_s), and the T_s dependences are markedly different as well.

These differences suggest that one (or both) of the experiments may involve artifacts. Several possibilities exist in these very difficult experiments. Certainly the authors are the most competent to judge and discuss these possibilities. However, we here point out some of our own concerns. Kolasinski et al. do report that a sizable coverage of O atoms builds up on the surface during the sticking measurements. If S at the O impurities is much larger than S on the bare surface, then the sticking observed by them could be dominated by these impurities and have a very different behavior than on the bare surface. On the other hand, the experiments by Höfer and co-workers relied on a somewhat indirect method for measuring sticking, i.e., monitoring the H coverage on the Si(100) surface via second harmonic generation of 1.06 μm radiation when the surface is in contact with H_2 or D_2 gas. However, there is no good theoretical model for the intensity of the second harmonic signal $I_{2\omega}$ at Si(100) surfaces. It is presumably related in some way to the density of dangling bonds at the surface and not strictly to H coverage, so that $I_{2\omega}$ may also be sensitive to defect density as well. It was shown by Bratu and Höfer[17] that a reduction of $I_{2\omega}$ is proportional to H coverage at one T_s. However, sticking studies probe a wide range of T_s, and it is likely that the defects, both on the bare surface and H induced,[31] are also strongly T_s dependence. In such a case, all the T_s dependence observed by Bratu and Höfer may not be due to changes in H coverage. They did not, for example, show that the same proportionality constant relating H coverage to $I_{2\omega}$

exists at all T_s, so that a contribution to $I_{2\omega}$ from defects could be excluded.

The calculations presented in Figs. 8–10 are not in qualitative accord with either experiment. The strong exponential increase of S with E_i predicted in the sub-barrier region (low E_i) is at odds with the weak E_i dependence observed by Kolasinski et al. Also, although the weak T_s dependence is in reasonable accord with the experiments of Kolasinski et al., this behavior is in marked disagreement with the very strong T_s dependence of Höfer and co-workers. We discuss in Sec. VIII C several possible sources for the disagreement between the dynamical calculations and the experiments.

B. Desorption

The quite large final translational energies for the desorbing D_2 predicted for both the asymmetric and symmetric paths ($\langle E_f \rangle = 0.45$ and 0.63 eV, respectively) are in strong qualitative disagreement with the experiment of Kolasinski et al.[14] who find $\langle E_f \rangle = 0.077 \pm 0.08$ eV. Possible rationales for this disagreement are discussed in the next section. The modest vibrational excitation predicted for desorption through either transition state is in qualitative agreement with the experimental value $P_{v=1} = 0.08$,[13] although slightly overestimated.

C. Possible sources of disagreement

The absence of agreement between the dynamical model presented here and the experiments could arise from several sources; experimental artifacts, a wrong ab initio (and hence model) PES, if a three-dimensional model is not sufficient to capture the essential dynamics or if the physics of dissociation desorption on real surfaces is not governed by a mechanism of adiabatic desorption through the "prepared" species.

The possibilities for experimental difficulties have been discussed earlier, and without further measurements it is impossible to judge the plausibility of this. We do note, however, that sticking probabilities are quite small and therefore very susceptible to problems associated with contaminants and defects. In principal, the desorption measurements should be less sensitive to these. However, if some types of defects are mobil, then defect mediated desorption could also be important. One theoretical study[6] has suggested a desorption mechanism based on rapid migration of unpaired surface Si defects and ultimate desorption from a dihydride species formed by H reaction at the defect.

While we can never prove that the PES used in the dynamics is qualitatively correct, we do point out that several recent density functional calculations (DFT) using generalized gradient corrections to the functional (GGA) all produce similar qualitative PES. These include both cluster[9] and slab models[10–12] of the surface. There is no way in general to guarantee that the GGA approximation in DFT produces a qualitatively correct PES without going beyond this level of approximation, which is currently impossible for surface calculations. We should point out that for H_2 elimination barri-

ers from small silane molecules, different functionals in DFT produce somewhat different results (by several tenths of eV), and these differ somewhat from those obtained via traditional quantum chemistry calculations (CI).[32] However, DFT calculations with the GGA do produce PES in agreement with experiment for the dissociation of H_2 on Cu(111) and other surfaces.[33,34] While there are slight differences in the magnitude of the barriers for the different calculations (typically <0.2 eV) associated with the different surface models, they still all predict qualitatively similar PES and hence dynamic couplings. There is thus no compelling reason to suspect that the PES used here do not qualitatively describe the minima energy path for dissociation and desorption, although the absolute magnitude of the theoretical barrier may be slightly suspect.

We can also not prove *a priori* that this reduced dimensionality model captures the essence of the dynamics. Although the PES contains full relaxation of all coordinates, the dynamical model is based on assuming three "active" coordinates, Z, D and a single Si phonon mode. The restriction to only two molecular coordinates Z and D has a long and successful history in dynamical models of H_2 dissociation on metals.[35] There are several phonon modes for the Si(100) surface.[36] From the *ab initio* PES, the mode that seems to be most strongly coupled to the reaction coordinate is the dimer tilt. We have therefore described the full relaxation of the Si lattice upon reaction in terms of this one phonon. We anticipate that the most important aspect of the phonon coupling is to be able to describe the average energy transfer to the lattice around the minimum energy path, and this should be well represented by a single phonon coordinate.[27] However, there is certainly no way to guarantee that other aspects of the phonon coupling or other modes, e.g., those involving in plane Si–Si stretches, are not important as well.

As discussed before, the possible role of defects in the dissociation and desorption dynamics cannot be fully excluded. If this is true, then our model of dynamics via a pre-paired species may not be at all relevant to the experiments to date. Whether this is a problem of experimental artifact or inappropriate physical model is then largely a matter of bias. In fact, several authors[4–6] have argued on the basis of *ab initio* cluster calculations that the pre-pairing mechanism is not the dominant mechanism. Our calculations certainly do not confirm the pre-pairing mechanism. On the other hand, because of all the uncertainties in both the experiments and the theoretical model, we do not feel it can be excluded either. Another issue, however, is whether doping of the semiconductors plays any role in the dynamics. The PES is appropriate for a fully undoped sample with a Fermi level at midgap. However, experiments have been performed on highly doped samples where there is substantial band bending for the bare surface. When this occurs, there is an associated electric field at the surface. *Ab initio* calculations[37] have shown a sensitivity of H adsorption energies, and therefore probably the barrier height for dissociation/desorption, to electric field. Thus, it is possible that barrier heights calculated for the undoped sample are not

relevant for the experimental situation. An even more fundamental issue is whether an electronically adiabatic model is appropriate at all for describing the dynamics when doping is present.[38] The lowest energy state with H_2 or D_2 far from the surface is one where the Si(100) energy (relative to the vacuum level) is shifted by band bending caused by charge transfer to or from dopants to the surface state. On the monohydride surface, surface states are quenched and the lowest energy state is one in which there is no band bending at the surface. In a diabatic representation, where electron transfer between dopants and the surface state is frozen, a curve crossing must exist. The adiabatic dynamical limit, discussed in this paper, only occurs when this electron transfer rate is extremely fast compared to the time scale of dissociation/ desorption. Since transfer from dopants at significant depths in the bulk is required to establish band bending, there is no guarantee that such an adiabatic picture is entirely correct. Carefully controlled dissociation and desorption experiments as a function of doping level will be required to see if any of these possible effects due to dopants is important. Alternatively, the effects of laser irradiation of the surface on sticking/desorption could also probe whether such electronic effects are important.[39]

IX. SUMMARY AND CONCLUSIONS

We report here dynamical simulations for dissociative chemisorption and associative desorption of D_2 on Si(100). We have shown in the appendix how to reduce the multidimensional dynamical problem to a reduced dimensionality one in terms of "active" coordinates. This procedure defines the dynamically relevant effective potentials U_{eff} to be used in the simulations. For the calculations reported here U_{eff} were obtained from *ab initio* PESs involving the pre-paired species. All calculations were carried out for two paths or transition states; an asymmetric one and a symmetric one. Quantum wavepacket dynamics was used for dissociative chemisorption and (principally) quasiclassical dynamics for associative desorption. The quantum simulations demonstrate that neither dissociation nor desorption are dominated by tunneling under any of the relevant experimental conditions.

Predictions for dissociative chemisorption are qualitatively similar, but quantitatively different, through both the asymmetric and symmetric transition states. Both show an initial very strong roughly exponential rise of dissociation probability with increasing energy in the sub-barrier region due to tunneling, followed by a slow approach to the asymptotic high energy limit for incident energies above the barrier. Both also predict quite weak increases of S with surface temperature. The latter is taken as evidence of rather weak dynamic coupling in the dissociation to the Si(100) dimer phonon mode and this can be rationalized in terms of the PES. The coupling is weak enough for the symmetric path that a "sudden" approximation is valid for the phonon coordinate, but the energy transfer is sufficient in the asymmetric path that such a "sudden" approximation is not a very good description of the dynamics. Although energetics favors the

asymmetric path, phase space (and higher T_s) favor the symmetric path so that both could be important in dissociative chemisorption and desorption.

Simulations of associative desorption predict that D_2 desorbs with considerable excess translational energy, both for the asymmetric and symmetric paths. There is in fact very little energy transfer from translation to the lattice upon desorption. The D_2 is predicted to desorb with some vibrational excitation, however.

Several models have previously been proposed to account for experimental observations on H_2 or D_2 dissociation and desorption from Si(100). Although our calculations include most of these effects, we cannot corroborate the implicit assumptions which are the basis of these models. "Entropic" barriers do cause a large reduction in S, but do not result in a slow increase of S with incident energy as suggested previously.[15] Such entropic barriers, obtained via static multidimensional extensions of the three dimensional dynamics, do not therefore resolve the apparent violation of detailed balance obtained when comparing adsorption and desorption barriers from experiments. The coupling of the reaction to the lattice found in dynamics based on the *ab initio* PES is also much smaller than that of models assuming an *ad hoc* PES, and suggests that the coupling to the lattice is also not the resolution of the apparent violation of detailed balance.

In summary, the results of this purely *ab initio* model of D_2 dissociation and desorption through the pre-paired dimer of Si(100) is in poor agreement with several experiments. Several reasons for this are discussed; experimental artifact, limitations in the theory, importance of impurity doping and the possibility that the experimental situation is not dominated by adiabatic processes through the pre-paired species.

ACKNOWLEDGMENTS

APPENDIX

1. Reduced dimensionality dynamical models

Within the Born–Oppenheimer approximation, the time evolution of a system is given rigorously in terms of multidimensional dynamics on a potential energy surface (PES). Thus, the electronically adiabatic dissociative chemisorption and associative desorption of D_2 on Si(100) is fully described in terms of such dynamics. Unfortunately, for such a description to be rigorous requires many modes. It is hence imperative to reduce the dimensionality in the dynamic description by making reasonable approximations. The success of the

dynamic description then depends on how well a limited number of coordinates describe the full time evolution.

In this Appendix, we briefly sketch a formal definition of a reduced dimensionality dynamical model for dissociative chemisorption and associative desorption. Such a formal definition is imperative in order to treat properly the dynamical implications of the neglected coordinates. Our definition is similar to so-called "reaction surface" descriptions of gas phase dynamical problems,[40] e.g. multidimensional intramolecular tunneling, and is in some ways a generalization of the reaction path formalism traditionally used in chemical dynamics.

We assume that the full dimensionality of the problem is described in terms of two classes of internal coordinates; "active" coordinates $\mathbf{r}$ that are strongly involved in the reaction and "spectator" coordinates $\mathbf{q}$ which are assumed to couple only weakly in the reaction. A reaction surface is defined by minimizing the total potential subject to the constraint of fixed $\mathbf{r}$:

$$\frac{\partial V(\mathbf{r},\mathbf{q})}{\partial \mathbf{q}} = 0. \tag{A1}$$

The values of $\mathbf{q}$ determined by this equation for a given $\mathbf{r}$ are denoted by $\mathbf{q}_0$. Note that this is the potential provided in *ab initio* electron structure calculations when producing PES grids in the coordinates $\mathbf{r}$ when all of the other coordinates are fully relaxed.

The full potential energy $V(\mathbf{r},\mathbf{q})$ can then be approximated by a Taylor series expansion of the $\mathbf{q}$ dependence to second order.

$$V(\mathbf{r},\mathbf{q}) = V[\mathbf{r},\mathbf{q}_0(\mathbf{r})] + \tfrac{1}{2}[\mathbf{q}-\mathbf{q}_0]\mathbf{F}(\mathbf{r})[\mathbf{q}-\mathbf{q}_0], \tag{A2}$$

where the elements of the force constant matrix $\mathbf{F}(\mathbf{r})$ are given as

$$F_{i,j}(\mathbf{r}) = \left(\frac{\partial^2 V(\mathbf{r},\mathbf{q})}{\partial q_i\,\partial q_j}\right)_{\mathbf{q}=\mathbf{q}_0(\mathbf{r})}. \tag{A3}$$

Transforming the $\mathbf{q}$ coordinates to normal coordinates $\mathbf{Q}$ it can be shown[40] that the classical Hamiltonian can then be approximated to quadratic expansion in $\mathbf{Q}$ as

$$H(\mathbf{r},\mathbf{P_r},\mathbf{Q},\mathbf{P_Q}) = H_r(\mathbf{r},\mathbf{P_r}) + H_{\text{vib}}(\mathbf{Q},\mathbf{P_Q};\mathbf{r}), \tag{A4}$$

where $\mathbf{P_r}$ and $\mathbf{P_Q}$ are the momenta conjugate to $\mathbf{r}$ and $\mathbf{Q}$. H_r is the usual Hamiltonian in terms of the "active" coordinates (assuming all spectator coordinates relaxed):

$$H(\mathbf{r},\mathbf{P_r}) = \tfrac{1}{2}\mathbf{P_r}\cdot\mathbf{G_{rr}}\cdot\mathbf{P_r} + V[\mathbf{r},\mathbf{q}_0(\mathbf{r})]. \tag{A5}$$

The elements $\mathbf{G_{rr}}$ are the usual Wilson $\mathbf{G}$ matrix elements describing the kinetic energy in terms of internal coordinates $\mathbf{r}$. H_{vib} is the vibrational Hamiltonian for all the "spectator" coordinates and which depends parametrically on the values of $\mathbf{r}$:

$$H_{\text{vib}}(\mathbf{Q},\mathbf{P_Q};\mathbf{r}) = \tfrac{1}{2}\mathbf{P_Q}\cdot\mathbf{P_Q} + \tfrac{1}{2}\mathbf{Q}\cdot\omega^2(\mathbf{r})\cdot\mathbf{Q}, \tag{A6}$$

$\omega(\mathbf{r})$ are the normal mode frequencies for the "spectator" modes about the minima and which depend parametrically on $\mathbf{r}$.

In a direct product basis set $\Psi(\mathbf{r},\mathbf{Q})=\psi(\mathbf{r})\phi(\mathbf{Q};\mathbf{r})$, the quantum mechanical Hamiltonian is represented by adiabatic channels diagonal in $\mathbf{Q}$ (with quantum numbers $\mathbf{n}$)

$$H(\mathbf{r},\mathbf{P_r},\mathbf{Q},\mathbf{P_Q})=H_n(\mathbf{r},\mathbf{P_r})=H_r(\mathbf{r},\mathbf{P_r})+(\mathbf{n}+\tfrac{1}{2})\cdot\hbar\,\omega(\mathbf{r}).$$
$$(A7)$$

and nonadiabatic terms off diagonal in $\mathbf{Q}$ which are proportional to $\langle\phi_{n'}|(\partial\phi_n/\partial\mathbf{r})\rangle$.

Neglecting the nonadiabatic terms [valid when $\partial\ln\omega_k(\mathbf{r})/\partial\mathbf{r}$ for all normal modes k is negligible], the Hamiltonian becomes for the ground state $\mathbf{n}=0$,

$$H_0(\mathbf{r},\mathbf{P_r})=H_r(\mathbf{r},\mathbf{P_r})+\tfrac{1}{2}\Sigma\hbar\,\omega_k(\mathbf{r}),\qquad(A8)$$

where the sum is over the normal modes $\mathbf{Q}$. The role of the "spectator" coordinates is then simply included in the reduced dimensionality model by using an effective potential

$$U_{\text{eff}}(\mathbf{r})=V[\mathbf{r},\mathbf{q_0}(\mathbf{r})]+\tfrac{1}{2}\Sigma\hbar\,\omega_k(\mathbf{r}).\qquad(A9)$$

This is of course the usual zero point corrected effective potential. At the saddle point, this effective potential yields the barrier familiar in transition state theory. The use of this $U_{\text{eff}}(\mathbf{r})$ then represents the "best" allowance for the "spectator" coordinates in a pure reduced dimensionality model.

2. Multidimensionality

In this section we discuss approximate methods to reintroduce effects of the "spectator" coordinates in more detail, e.g., to describe the vibrational phase space associated with these modes. The full multidimensional Hamiltonian is represented by a set of adiabatic channels, Eq. (A7), coupled by nonadiabatic terms. Assuming that the nonadiabatic terms are weak compared to the differences in adiabatic channel energies, then the full dynamical solution S_{nd} can be approximated as

$$S_{nd}\approx A^{-1}\Sigma_{\mathbf{n}_i}P_{\mathbf{n}_i}S_{\mathbf{n}_i},\qquad(A10)$$

where $P_{\mathbf{n}_i}$ is the probability of being in the vibrationally adiabatic channel $\mathbf{n}_i$, $S_{\mathbf{n}_i}$ is the solution for the adiabatic channel $\mathbf{n}_i$ [equivalent to solving a reduced dimensionality problem with effective potential $V[\mathbf{r},\mathbf{q_0}(\mathbf{r})]+(\mathbf{n}_i+0.5)\hbar\,\omega_i(\mathbf{r})$] and A^{-1} is a normalization constant to make $S_{nd}=1$ at high incident energy. Equation (A10) assumes that the major role of the nonadiabatic terms is to induce transitions between adiabatic channels in some unspecified manner so that several channels are open. These open channels represent the vibrational phase space for the "spectator" modes.

Since the saddle point is the critical part of the PES defining dissociation and desorption, we take the normal coordinates $\mathbf{Q}$ to be those appropriate for $\mathbf{r}$ at the transition state. We also assume that the external modes, i.e., the hindered translations and rotations at the transition state, are most important. These modes adiabatically correlate with the low frequency modes in the asymptotic gas-surface region (molecular translation states parallel to the surface and molecular rotation) and hence can have appreciable weighting due to nonadiabatic mixing.

a. Dissociative adsorption

For a purely adiabatic dissociation (for normal incidence and for initial population only in the rotational ground state), $P_{\mathbf{n}_i=0}=1$ while all other $P_{\mathbf{n}_i}=0$. Only the lowest adiabatic channel contributes to the dissociation and the reduced dimensionality model with U_{eff} represents fully the effects of higher dimensionality. This adiabatic limit describes complete "steering" to the minimum energy configuration in $\mathbf{Q}$ and is most appropriate when $\omega_k^{\pm}\gg\tau_c^{-1}$, where $\omega_k^{\pm}$ are the external frequencies at the transition state and τ_c^{-1} is the collision time.

The opposite extreme occurs when there is complete mixing of the adiabatic channels. In this case, all accessible channels N are assumed populated with equal probability $P_{\mathbf{n}_i}=1/N$. This weighting corresponds to the complete absence of "steering" and is most relevant when $\omega_k^{\pm}\ll\tau_c^{-1}$. Unfortunately, N is rather ill defined. In any event, when the nonadiabatic transitions are so strong as to mix stochastically the adiabatic channels, it is probably more appropriate to utilize a diabatic formulation. A classical analog of this diabatic formulation is contained in the familiar "hole" model[41,42] and which consistently treats the multidimensionality in this limit via a sudden approximation.

For the region between the two extremes, we simply assume that

$$P_{\mathbf{n}_i}\propto(1/N)e^{-\xi\mathbf{n}_i}\qquad(A11)$$

provides a reasonable interpolation by varying ξ. This allows for flexibility in the degree of "steering". As N, we take the maximum number of harmonic states at the transition state allowed in the absence of steering.

If we assume that only changes in the barrier height δU determine the overall dissociation probability, then $S_{\mathbf{n}_i}$ can be approximated statically as

$$S_{\mathbf{n}_i}(E)=S_0(E-\alpha\,\delta U_{\mathbf{n}_i}),\qquad(A12)$$

where S_0 refers to the $\mathbf{n}=0$ solution, $\delta U_{\mathbf{n}_i}$ is the change of the barrier height for the adiabatic channel $\mathbf{n}_i$. α is approximately the change in the classical threshold of the state of $H_0(\mathbf{r})$ with barrier height variation[26] and E is the incident energy. These approximations produce a rigid shift of the excitation profile with changes in barrier height. Note that this static approximation can also be used to estimate the effects of a different effective potential barrier $(U+\delta U)$ on the dynamics when dynamical calculations already exist for another barrier height (U), i.e.,

$$S(E;U+\delta U)\approx S(E-\alpha\,\delta U;U).\qquad(A13)$$

Combining both definitions, we find that Eq. (A10) is given as

$$S_{7d}(E)=(1/N)A^{-1}\Sigma_{\mathbf{n}_i}e^{-\xi\mathbf{n}_i}S_{3d}(E-\alpha\,\delta U_{\mathbf{n}_i}).\qquad(A14)$$

b. Associative desorption

For associative desorption, Eq. (A10) becomes

$$P_{\text{des}}=A^{-1}\Sigma_{\mathbf{n}_i}P_{\mathbf{n}_i}S_{\text{des}}(\mathbf{n_i}),\qquad(A15)$$

where P_{des} is the total desorption probability. It is assumed that on the surface side of the barrier all channels are strongly coupled and thermally populated. However, after passing through the transition state, there is only weak coupling as the molecule desorbs into the gas phase and we can then consider separate adiabatic channels populated at the transition state, i.e., $P_{\mathbf{n}_i} \propto e^{-\hbar \omega_{\mathbf{n}_i}^{\pm}/kT_s}$ where $\omega_{\mathbf{n}_i}^{\pm}$ are the frequencies at the transition state. Under these conditions, the multidimensional rate k_{des} is given by transition state theory [assuming $S_{des}(n_i^+) \equiv 1$].

[1] K. Sinniah, M. G. Sherman, L. B. Lewis, W. H. Weinberg, J. T. Yates, Jr., and K. C. Janda, Phys. Rev. Lett. **62**, 567 (1989).

[2] U. Höfer, L. Li, and T. F. Heinz, Phys. Rev. B **45**, 9485 (1992).

[3] M. P. D'Evelyn, Y. L. Yang, and L. F. Sutcu, J. Chem. Phys. **96**, 852 (1992).

[4] C. J. Wu, I. V. Ionova, and E. A. Carter, Surf. Sci. **295**, 64 (1993).

[5] Z. Jing and J. L. Whitten, J. Chem. Phys. **98**, 7466 (1993); Z. Jing and J. Whitten, *ibid*. **102**, 3867 (1995).

[6] P. Nachtigall, K. D. Jordan, and C. Sosa, J. Chem. Phys. **101**, 8073 (1994).

[7] P. Nachtigall, K. D. Jordan, and K. C. Janda, J. Chem. Phys. **95**, 8652 (1991).

[8] P. Nachtigall, C. Sosa, and K. D. Jordan, J. Phys. Chem. **97**, 11 666 (1993).

[9] S. Pai and D. Doren, J. Chem. Phys. **103**, 1232 (1995).

[10] P. Kratzer, B. Hammer, and J. K. Nørskov, Chem. Phys. Lett. **229**, 645 (1994).

[11] E. Pehlke and M. Scheffler, Phys. Rev. Lett. **74**, 952 (1995).

[12] A. Vittadini and A. Selloni, Chem. Phys. Lett. **235**, 334 (1995).

[13] K. W. Kolasinski, S. F. Shane, and R. N. Zare, J. Chem. Phys. **96**, 3995 (1992).

[14] K. W. Kolasinski, W. Nessler, A. de Meijere, and E. Hasselbrink, Phys. Rev. Lett. **72**, 1356 (1994).

[15] K. W. Kolasinski, W. Nessler, K.-H. Bornscheuer, and E. Hasselbrink, J. Chem. Phys. **101**, 7082 (1994).

[16] M. Liehr, C. M. Greenlief, M. Offenberg, and S. R. Kasi, J. Vac. Sci. Technol. A **8**, 2960 (1990).

[17] P. Bratu and U. Höfer, Phys. Rev. Lett. **74**, 1625 (1995).

[18] W. Brenig, T. Brunner, A. Gross, and R. Russ, Z. Phys. B **93**, 91 (1993).

[19] P. Bratu, K. L. Kompa, and U. Höfer, Chem. Phys. Lett. (in press).

[20] P. Bratu, W. Brenig, A. Gross, U. Höfer, P. Kratzer, and R. Russ. 1995, to be published.

[21] W. Brenig, A. Gross, and R. Russ, Z. Phys. B **96**, 231 (1994).

[22] E. Pehlke and M. Scheffler, in *Proceedings of the 22nd International Conference on the Physics of Semiconductors*, edited by D. Lockwood (World Scientific, Singapore, 1994).

[23] P. Kratzer, B. Hammer, and J. K. Nørskov, Phys. Rev. B **51**, 13432 (1995).

[24] H. Weinberg, in *Dynamics of Gas-Surface Collisions*, edited by M. N. R. Ashford and C. T. Rettner (Roy. Soc. Cem., Cambridge, 1991).

[25] J. P. Perdew, J. A. Chevary, S. H. Vosko, K. A. Jackson, M. R. Pederson, D. J. Singh, and C. Fiolhais, Phys. Rev. B **64**, 6671 (1992).

[26] A. C. Luntz, J. Chem. Phys. **102**, 8264 (1995).

[27] A. C. Luntz and J. Harris, Surf. Sci. **258**, 397 (1991).

[28] M. R. Hand and S. Holloway, J. Chem. Phys. **91**, 7209 (1989).

[29] P. Kratzer, R. Russ and W. Brenig, Surf. Sci. (in press).

[30] J. Harris, S. Holloway, T. Raman, and K. Yang, J. Chem. Phys. **89**, 4427 (1988).

[31] F. Owman and P. Martensson, Surf. Sci. **324**, 211 (1995).

[32] P. Nachtigall, K. D. Jordan, A. Smith, and H. Johnson, J. Chem. Phys. (submitted).

[33] B. Hammer, K. W. Jacobsen, and J. K. Nørskov, Phys. Rev. Lett. **70**, 3971 (1993).

[34] B. Hammer, M. Scheffler, K. W. Jacobsen, and J. K. Nørskov, Phys. Rev. Lett. **73**, 1400 (1994).

[35] U. Nielsen, D. Halstead, S. Holloway, and J. K. Nørskov, J. Chem. Phys. **93**, 2879 (1990).

[36] D. C. Allan and E. J. Mele, Phys. Rev. Lett. **53**, 826 (1984).

[37] P. Kratzer, B. Hammer, F. Grey, and J. K. Nørskov, Phys. Rev B. (submitted).

[38] P. Kratzer, B. Hammer, and J. K. Nørskov (unpublished).

[39] F. A. Houle, Phys. Rev. B **39**, 10120 (1989).

[40] T. Carrington, Jr. and W. H. Miller, J. Chem. Phys. **84**, 4364 (1986).

[41] M. Karikorpi, S. Holloway, N. Henriksen, and J. K. Nørskov, Surf. Sci. **179**, L41 (1987).

[42] K. Gundersen, K. Jacobsen, J. K. Nørskov, and B. Hammer, Surf. Sci. **304**, 131 (1994).